Influence of the initial setting of cement on the shear strength of rice husk ash stabilised soil

Najmun Nahar,[1,2] Alex Otieno Owino,[1] Zakaria Hossain[1]

[1]Department of Environmental Science and Technology, Faculty of Bioresources, Mie University, Tsu City, Mie, Japan; [2]Department of Geography and Environment, Faculty of Life and Earth Science, Jagannath University, Dhaka, Bangladesh

Abstract

Determination of soil shear strength is essential for engineering construction. Using rice husk ash (RHA) with cement in the soil is a potential ground improvement technique that can reduce environmental problems and construction budget. In the present study, ten combinations of soil-RHA-cement were investigated to understand the effects of RHA with cement on the shear strength parameters of the soil. The admixtures were prepared by taking soil with 5%, 10%, 15% RHA, and 2%, 4%, and 6% cement. All specimens of soil-RHA-cement were tested after the initial setting of cement. The direct shear test was set up to compare different soil-RHA-cement mixtures under three normal stresses of 40, 60, and 80 kPa. The test results showed the difference in each mixture's shear stress-shear displacement relationship, shear displacement-vertical displacement relationship, shear stress-normal stress relationship, shear strength, cohesion, and internal friction angle. According to the findings, shear strength improved as the cement ratio increased for the same amount of RHA in the soil, while dilatancy reduced compared to untreated soil. All soil-RHA-cement combinations had a stronger cohesiveness than untreated soil, but the angle of internal friction was lower. Under normal stress of 80 kPa, the soil with 5% RHA and 6% cement combination had the highest shear strength, corresponding to 62.9 kPa, and can be suggested for ground development.

Correspondence: Najmun Nahar, Department of Environmental Science and Technology, Faculty of Bioresources, Mie University, Tsu, Mie 514-8507, Japan.
Tel.: +81.90.9196.8981. E-mail: 519d2s3@m.mie-u.ac.jp; najmun_nahar33@yahoo.com

Key words: Chemical soil stabilisation; rice husk ash; shear behaviour; cohesion; friction angle.

Acknowledgements: the authors would like to acknowledge Ms. Hasegawa Rio for her assistance during the research at Mie University. The authors are grateful for the MEXT scholarship at Mie University, supported by the Japanese Ministry of Education, Culture, Sports, Science, and Technology. The authors are also indebted to Noma Tamaki, President of Make Integrated Technology (M.I.T.) company in Osaka, Japan, for providing research materials and financial support.

Contributions: NN, methodology, data curation, and original draft writing; AOW, manuscript review and editing; ZH, supervisor of the Ph.D. student, funding acquisition, and research coordination.

Conflict of interest: the authors declare no potential conflict of interest.

Received for publication: 18 March 2022.
Accepted for publication: 22 July 202.

Journal of Agricultural Engineering 2022; LIII:1411
doi:10.4081/jae.2022.1411

Introduction

Shear strength is the essential engineering attribute of soil because it determines how stable a soil mass is under structural stresses. It primarily defines the cohesion between soil particles and the interlocking or friction resistance of particles moving over each other (Dirgėlienė *et al*., 2017; Roy and Bhalla, 2017). The creation of shear stress in the soil mass due to loading or unloading caused by construction procedures accounts for the many failure modes of geotechnical engineering (Eslami *et al*., 2019). Consequently, soil stabilisation is required to improve untreated soil's shear strength (cohesion and angle of internal friction), which is fundamental for foundation engineers to design various geotechnical constructions. Cement has been one of the most common additives in soil stabilisation for many years. Many environmental scientists have suggested using supplementary cementitious materials, which can reduce the use of cement in construction industries, considering the environmental pollution during cement production. The common waste materials from agricultural sectors are coconut shells ash, palm oil fuel ash, rice husk ash, sugarcane bagasse ash, *etc*. (Gunasekaran *et al*., 2013). Over the years, rice husk ash (RHA) waste, the agricultural bi-product, has been a popular pozzolanic material that contains the highest reactive amorphous silica (85-95%) among all agricultural wastes (Basha *et al*., 2005; Jamil *et al*., 2013; Thomas, 2018). Therefore, it can reduce cement usage in construction (Alhassan and Alhaji, 2017; Jongpradist *et al*., 2018), which is also economically and environmentally viable (Khan *et al*., 2012). Additionally, RHA and cement added to the soil enhanced its permeability (Nahar *et al*., 2021), indicating the needlessness of preventative soil treatment. Many studies have already investigated the effects of RHA and cement with soil for ground improvement through various

laboratory tests. For laterite soil mixed with RHA and cement, Rahman (1987) performed the Atterberg limit test, compaction test, unconfined compressive strength (UCS) test, and California bearing ratio (CBR) test. The compaction properties, UCS, and durability of residual sandy clay soil were studied by Ali *et al*. (1992). Basha *et al*. (2005) and Khan *et al*. (2016) carried out the Atterberg limit test, compaction test, UCS test, and CBR test for residual soil improvement. Kaur and Jha (2016) and Jongpradist (2018) assessed clayey soil's compaction properties and UCS. The Atterberg limit test and the UCS test for borehole soil were done by Nguyen and Nguyen (2020). A direct shear test was used in a few studies to determine the cohesiveness and angle of internal friction of soil-RHA-cement combinations. Only Eliaslankaran (2021) conducted a direct shear test under 500 kPa normal stress and a UCS test where RHA was individually added with cement and lime at varied ratios considering 7, 14, 28, and 90 days of curing to understand the strength properties of coastal silty sand. In addition, to the best of the authors' knowledge, no effort has been made to use direct shear testing to examine the effects of initial cement setting on the shear strength of RHA-stabilised soil.

In light of the discussion above, the present study investigated the shear behaviour of several soil-RHA-cement combinations during initial cement setting through direct shear testing. As an essential parameter of soil, foundation and geotechnical engineers always apply the idea of shear strength for the stability of agricultural structures, embankments, slopes, road construction, retaining walls, airfield pavements, *etc*. Therefore, the direct shear tests were performed for this investigation under 40, 60, and 80 kPa normal stresses. Furthermore, for a better understanding of the shear behaviour of soil, the shear stress-shear displacement relationship, vertical-horizontal displacement relationship (dilatancy behavior), shear strength-normal stresses curves were illustrated, and cohesion and angle of internal friction soil-RHA-cement mix types were calculated in this study.

Materials and methods

Materials used

Soil, as-obtained rice husk ash (RHA), and ordinary Portland cement (OPC) were used as the materials of this study. The soil sample was taken in the Handa area in Tsu City, Mie Prefecture, Japan. A construction company collected soil samples taken from the foothill at a depth of within 3 meters. The pressure was within the ratio of over-consolidation. After drying in a room, the soil was sieved through a US 8 No. Sieve (2.38 mm). There was no organic matter in the soil. The specific gravity of the soil was 2.7. The soil had 17.5% optimum moisture content and a maximum dry density of 1.696 g/cm^3. The particle size distribution curve of soil (Figure 1A) revealed that the soil was well graded, as the coefficients of curvature (C_c) and coefficients of gradation (C_u) were 1.024 and 9.841, respectively. The plasticity index of the soil was 7.8%. The soil is classified as silty sand per the Unified Soil Classification System (USCS) and SM soil based on the American Association of State Highway and Transportation Officials (AASHTO) classification. The Make Integrated Technology (M.I.T.) company provided the ready-obtained RHA in Osaka, Japan. The RHA was produced after burning at 650°-700°C temperature for 27 hours. The RHA was medium to fine-textured (0.075 to 0.85 mm), as observed by the RHA particle size distribution curve (Figure 1B). The specific gravity of RHA was 2.12 g/cm^3. The RHA was composed of 91.10% amorphous silica (SiO_2), 0.57% calcium oxide (CaO), 0.03% alumina (Al_2O_3), and 4.35% carbon dioxide (CO_2). The properties of ordinary Portland cement are available in other studies (Lee *et al*., 2014).

Mix designs and preparation of the specimens

Specimens of soil-RHA-cement combinations containing 5%, 10%, 15% RHA, and 2%, 4%, and 6% cement were used for this study. Table 1 shows the various soil-RHA-cement mix types and their optimum moisture content (OMC). Each admixture's OMC was assessed before adding water to the soil-RHA-cement admixtures. About 2% water was removed from OMC for better cement hydration in the admixtures. The specimens were tested after 30 minutes during the initial setting stage of cement with water in the soil-RHA mixture.

Testing procedures

The direct shear test was carried out for this investigation. The testing procedure of this test is relatively easy, but it is not directly related to field condition, and the stress distribution is not uniform on the failure plane (Murthy, 2002). To understand the shear behaviour of soil-RHA-cement combination types, the direct shear test was performed according to the Japanese Geotechnical Society (JGS 0561, 2010). The test was conducted at the drained condition under constant normal stress of 40 kPa, 60 kPa, and 80 kPa. The shear box has two parts, a fixed lower box, and a moving upper shear box, with a similar size of 50 mm depth. During the test, four sidewalls and their girder control the mobility of soil parallel to the

Table 1. Mixing indices of soil-rice husk ash-cement combination types.

Soil no.	Mix types	Index	OMC (%)
1	Soil (Control)	Control	17.5
2	Soil + 5% RHA + 2% Cement	S+5R+2C	21.2
3	Soil + 5% RHA + 4% Cement	S+5R+4C	21.6
4	Soil + 5% RHA + 6% Cement	S+5R+6C	22.0
5	Soil + 10% RHA + 2% Cement	S+10R+2C	25.0
6	Soil + 10% RHA + 4% Cement	S+10R+4C	25.5
7	Soil + 10% RHA + 6% Cement	S+10R+6C	26.1
8	Soil + 15% RHA + 2% Cement	S+15R+2C	29.3
9	Soil + 15% RHA + 4% Cement	S+15R+4C	30.1
10	Soil + 15% RHA + 6% Cement	S+15R+6C	30.6

OMC, optimum moisture content; RHA, rice husk ash.

shear surface, which is mainly constructed for this apparatus. The normal stress is applied through a lower jack below the lower box, balanced by the upper box's opposite stresses. On the outside, the shear box with a clamping system has a rectangular shape of 150 mm in length, 100 mm in width, and 100 mm in height. The vertical screws set at both the long side of the upper box remove the friction between the upper box and the lower box.

In this test, computer software DCS-100 connected with a load cell, two dial-gauges have been used to record shear force data, horizontal and vertical displacement through one load cell, and two displacement transducers (one for shear displacement and the other for vertical measurement). Inside the shear box, samples were prepared and filled into three layers. With every test conducted, the same compaction energy was exerted for each layer to keep the density of the soil-RHA-cement admixtures consistent. Before performing the test, the consolidation was allowed for nearly 10 minutes by applying vertical load. After the consolidation by normal stresses was achieved, the shear load was applied through the screw jack. The screw jack is electrically operated at constant pressure with a 1.0 mm/min speed. During the test, normal stresses (vertical load) are kept stable. After applying a horizontal force to the upper half of the direct shear box, the specimens are sheared in half along a horizontal failure plane.

In this study, the shear stress *versus* horizontal displacement curves was drawn, and the maximum shear stress at each normal stress was determined. The soil cohesion and internal friction angle of each mixture can be obtained using the Coulomb failure criterion shown in Equation 1:

$$\tau_f = c + \sigma_f \tan \phi \quad (1)$$

where, τ_f is the shear strength of soil, c is the cohesion, σ_f is the normal stress on a plane, and ϕ is the angle of internal friction.

Results and discussion

Effects on shear stress-shear displacement and vertical displacement-shear displacement relationships

The shear stress-shear displacement and vertical displacement-shear displacement curves illustrate how shear behaviour affects the engineering aspects of soil. The shear stress (τ) *versus* shear displacement (u) and vertical displacement (v) *versus* shear displacement (u) in untreated soil is illustrated in Figure 1C and D correspondingly. According to the trend, the shear stress under normal stress began to be distinguished for the control specimen after reaching 0.5 mm horizontal displacement. The obtained maximum shear stresses of the control specimen were 22.7, 31.8, and 43.3 kPa for normal stresses of 40, 60, and 80 kPa, respectively (Figure 1C). A significant dilatancy (volumetric change) was observed for the vertical displacement-horizontal displacement curve under a normal load of 80 kPa. When the horizontal displacement was 7 mm, the vertical displacement peaked. The maximum vertical displacements were 2.10, 2.46, and 9.80 mm, corresponding to the normal stresses of 40, 60, and 80 kPa, respectively (Figure 1D).

The shear stress-shear displacement and vertical displacement-

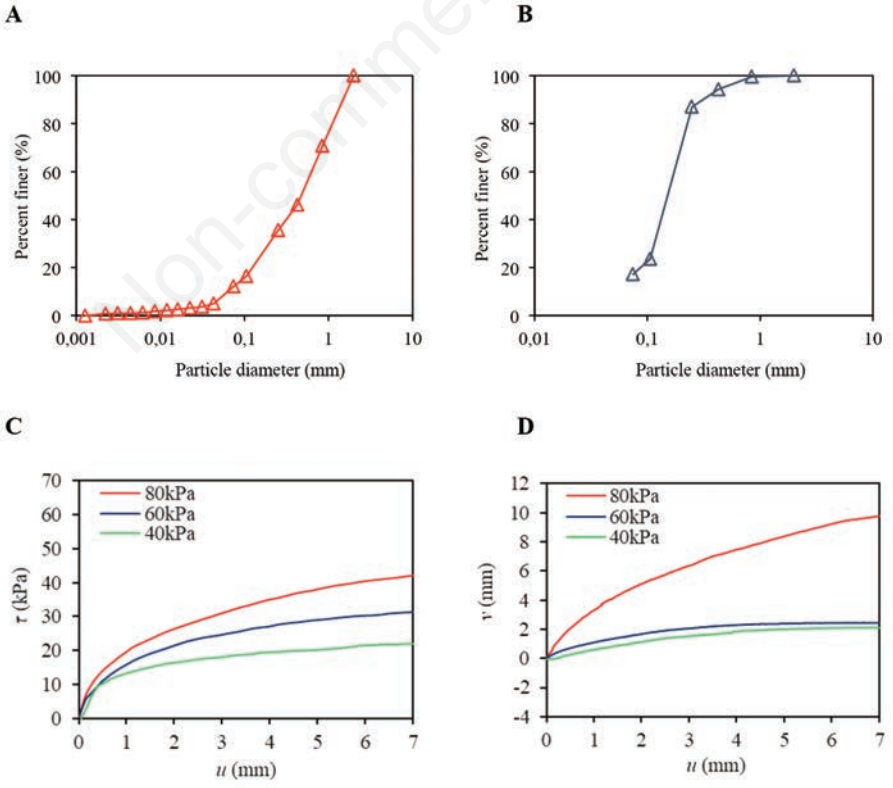

Figure 1. Particle size distribution curve of (A) soil and (B) RHA; C) shear stress (τ) *vs* shear displacement (u), and (D) vertical displacement (v) *vs* shear displacement (u) relationship of the control specimen.

shear displacement relationships of various soil-RHA-cement combinations under various normal stresses (40, 60, and 80 kPa) are exhibited in Figures 2-5 and 6A-B. From the beginning to the completion of the test, the shear stress between normal stresses 40 and 60 kPa for the S+5R+2C specimen was practically the same, as shown in Figure 2A. The specimen's dilatancy (volumetric change) is displayed in Figure 2B. A uniform volume change was observed for the S+5R+2C specimen. For the normal stress of 40 kPa, the dilatancy value of this admixture had a negative value from the initial to the end of the test, but positive dilatancy values were observed for the 60 and 80 kPa normal stresses mixture. Under normal loads of 40, 60, and 80 kPa, maximum shear stresses were 31.9, 33.9, and 40.7 kPa, and the highest vertical displacements were –0.23, 1.22, 3.99 mm, respectively, for the S+5R+2C combination.

The shear stress-shear displacement curves for 40 and 60 kPa in the specimen S+5R+4C followed a similar trend from 0-1.5 mm, then increased in parallel, but the curves for 60 and 80 kPa increased together up to 0.24 mm displacement, then improved separately until 4 mm, and then followed the same path until the end of the test (Figure 2C). With the increase of shear displacement, vertical displacement correspondingly increased with a constant volumetric change (Figure 2D). As a result, the maximum shear stress of the S+5R+4C was 35.9, 43.1, and 44.7 kPa, and the highest vertical displacement was 0.43, 1.37, and 2.34 mm under the normal stresses 40, 60, and 80 kPa correspondingly. For the specimen S+5R+6C, a constant horizontal displacement between 0-0.1423 mm was recorded under all normal stresses; afterward, the shear stress-shear displacement curves for 60 and 80 kPa together increased till 0.3462 mm, and later maintained the spacing between the curves under 60 and 80 kPa (Figure 3A). The volumetric change of this specimen was uniform and less significant due to the shear strength improvement of this specimen (Figure 3B). Among all soil-RHA-cement combination types, S+5R+6C showed the highest shear stress under all normal stresses. The maximum shear stress of this specimen was observed as 49.0, 60.1, and 62.9 kPa, and the uppermost vertical displacements were 0.99, 1.00, 1.00 mm for the normal stresses of 40, 60, and 90 kPa (Figure 3A and B).

Figure 3C and D represent the shear stress-shear displacement and shear displacement-vertical displacement curves for the S+10R+2C combination. The shear stresses for normal stresses 40 and 60 kPa were almost similar; both curves sharply increased with the displacement increase from 0 to 1 mm, then gradually increasing until the test's end. For normal stress of 80 kPa, shear stress increased together with 40 and 60 kPa curves from 0 to 0.1130 mm; after that increased differently and crossed the 40 and 60 kPa curves (Figure 3C).

Comparatively, a less volumetric change was detected for the vertical displacement of 40 kPa normal stress, but a tremendous volumetric change was observed for 60 and 80 kPa normal stresses. For the normal stress of 80 kPa, vertical displacement quickly fluctuated from 0 to 4.3179 mm (Figure 3D). The highest shear stresses of the S+10R+2C specimen were 25.4, 26.4, and 28.8 kPa, and the uppermost vertical displacements were 1.18, 4.44, and 8.66 mm individually.

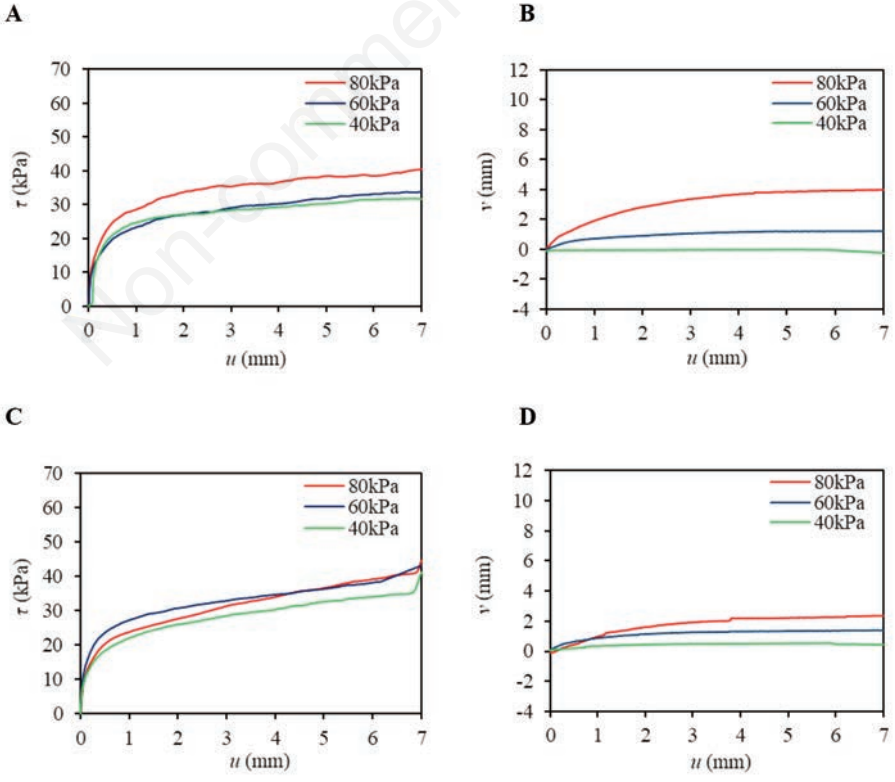

Figure 2. A) Shear stress (τ) *vs* shear displacement (u), and (B) vertical displacement (v) *vs* shear displacement (u) relationship of S+5R+2C specimen; C) shear stress (τ) *vs* shear displacement (u), and (D) vertical displacement (v) *vs* shear displacement (u) relationship of S+5R+4C specimen.

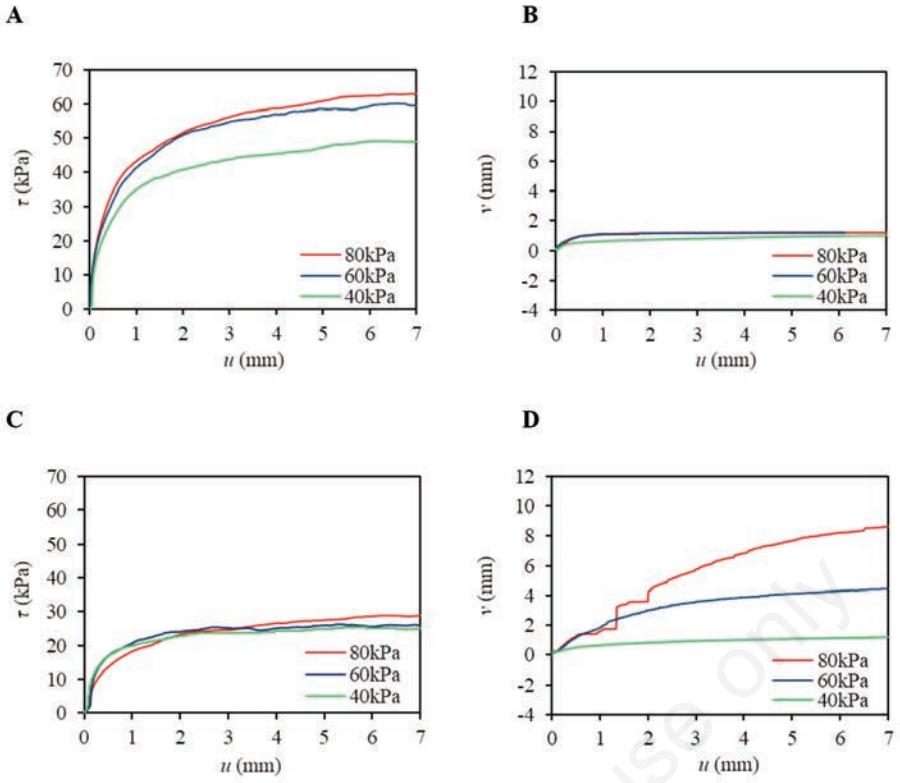

Figure 3. A) Shear stress (*τ*) *vs* shear displacement (*u*), and (B) vertical displacement (*v*) *vs* shear displacement (*u*) relationship of S+5R+6C specimen; C) shear stress (*τ*) *vs* shear displacement (*u*), and (D) vertical displacement (*v*) *vs* shear displacement (*u*) relationship of S+10R+2C specimen.

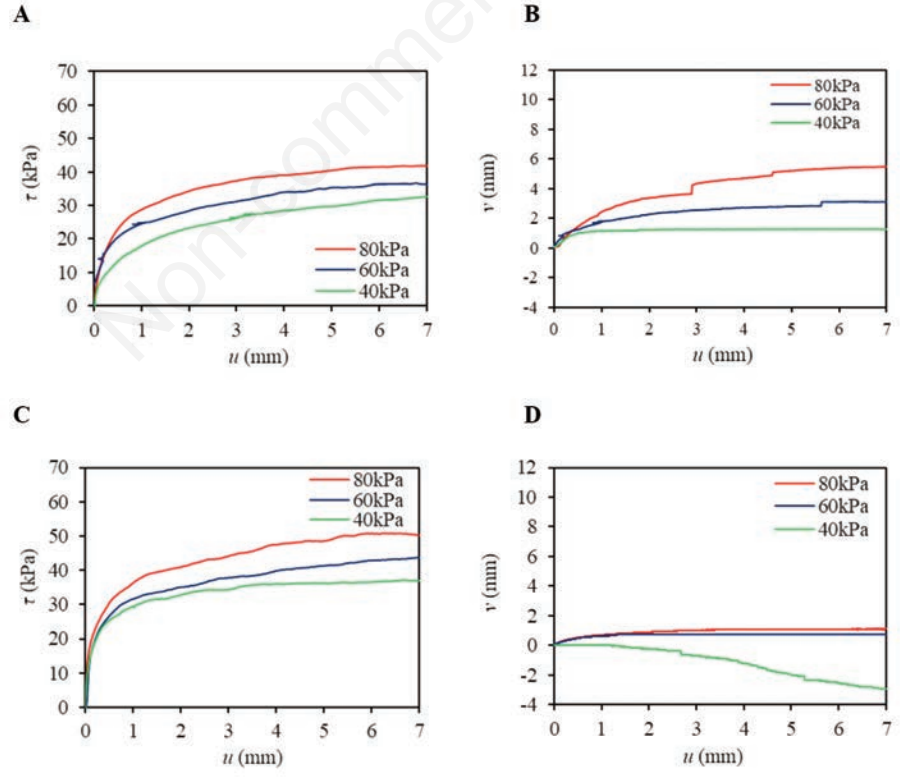

Figure 4. A) Shear stress (*τ*) *vs* shear displacement (*u*), and (B) vertical displacement (*v*) *vs* shear displacement (*u*) relationship of S+10R+4C specimen; C) shear stress (τ) *vs* shear displacement (*u*), and (D) vertical displacement (*v*) *vs* shear displacement (*u*) relationship of S+10R+6C specimen.

The shear stresses and vertical displacements of the S+10R+4C combination under normal stresses (40, 60, and 80 kPa) are illustrated in Figure 4A and B. Under all normal stresses, the S+10R+4C admixture followed very identical paths. The shear stress increased sharply with the increase of displacements from 0 to 1 mm for all normal stresses, then increased gradually following the same trend (Figure 4A). The vertical displacement for a 40 kPa normal stress was marginally higher than that of a 60 kPa normal stress and much higher than that of an 80 kPa normal stress (Figure 4B). For normal stresses 40, 60, and 80 kPa, the highest shear stress was 32.5, 36.7, and 42 kPa, and the maximum vertical displacement values were 1.23, 3.12, and 5.44 mm, respectively Figure 4C demonstrates the shear stress-shear displacement relationship, and Figure 4D illustrates the shear displacement-vertical displacement relationship curves of S+10R+6C under normal stresses 40, 60, and 80 kPa. Initially, from 0 to 0.2515 mm shear displacement, the shear stresses together increased quickly for all normal stresses (Figure 4B). A negative vertical displacement occurred as horizontal displacement increased for normal stress 40 kPa. Positive vertical displacement values were observed for 60 and 80 kPa, a less significant volumetric change (Figure 4B). The specimen's maximum shear stress was 37.1, 43.8, and 50.9 kPa, and the maximum vertical displacement values were –2.94, 0.74, 1.11 mm under 40, 60, and 80 kPa, respectively.

The shear stress-shear displacement curves for the combinations of S+15R+2C and S+10R+2C had a similar pattern, and the shear stress was not significantly increased with the increase of displacements and normal stresses (Figures 5A and 3C). A significant volumetric change was observed under 80 kPa normal stress for the specimen S+15R+2C (Figures 5B and 3D) due to the surplus amount of RHA with less cement in the soil. The highest vertical displacement value was observed from the S+15R+2C specimen for 80 kPa normal stress due to the high amount of RHA and the low amount of cement in the specimen (Figure 5B). For normal stresses 40, 60, and 80 kPa, ultimate shear stresses were 22.3, 24.7, and 25.4, and the uppermost vertical displacements were 0.96, 2.83, and 10.33 mm.

The shear stress-shear displacement curves of the S+15R+4C combination are shown in Figure 5C, and the relationship of the shear displacement-vertical displacement is illustrated in Figure 5D. Shear stress increased rapidly with the increment of shear displacement from 0 to 1 mm, and the shear stress-shear displacement curves were identical under all normal stresses. Less volumetric changes were detected for 40 kPa normal stress, but comparatively, high dilatancy values were observed for 60 and 80 kPa. The maximum shear stress of the specimen was 24.8, 26.9, and 36.7 kPa, and the maximum vertical displacement values were 1.17, 3.36, and 5.87 mm under normal stresses of 40, 60, and 80 kPa, respectively.

Figure 6A and B display the shear stress-shear displacement and shear displacement-vertical displacement curves of the S+15R+6C combination. The shear stress improved sharply from 0 to 0.08 mm displacement, grew slowly until 5.5 mm, and increased quickly until the test's end (Figure 6A). Due to the mixture's high cement content, volumetric changes were significant for 60 kPa and less significant for 40 and 80 kPa normal stresses. The maximum shear stress of the admixture was 36.7, 39.1, and 49.1 kPa, and the vertical displacement values were 0.40, 1.92, and 3.15 mm under stresses 40, 60, and 80 kPa, respectively.

In this study, the shear stress-shear displacement and vertical displacement-shear displacement relationships under normal stresses 40, 60, and 80 kPa were altered compared to the control specimen with the variation of RHA and cement ratios in soil-RHA-cement combinations considering the initial setting of cement (30 minutes). In most cases, shear stress improved as horizontal displacement increased (Choobbasti *et al*., 2010; Rachmawati *et al*., 2018), although the rate of increase also depends on the RHA and cement additive ratios for various normal stresses. Under all normal stresses, the shear stress increased abruptly from 0 to 1 mm horizontal displacement, then steadily increased for all soil-RHA-cement admixtures (Figures 2-5 and 6A-B). The S+5R+4C, S+5R+6C, S+10R+6C, and S+15+6C specimens showed higher shear stresses and minor deformation (volume change) under all normal stresses (40, 60, and 80 kPa) than the control specimen because a large concentration of cement with RHA accelerates the soil's flocculation process, resulting in a more brittle material. The higher dilatancy (volume changes) was observed for the S+10R+2C and S+15R+2C specimens than untreated soil under normal stress of 80 kPa due to the surplus amount of RHA and low amount of cement content.

Effects on shear strength

The relationship between shear strength and normal stresses is shown in Figure 6C. The shear strength of the specimens of S+5R+4C, S+5R+6C, S+10R+6C, and S+15+6C was higher than the control specimen. Shear strength may have enhanced due to the rapid agglomeration of unsettled RHA and cement particles with water into micro flocs and bulky flocs in the soil. Following the initial setting of cement, shear strength improvement was also attributable to cement hydration in the RHA mixed soil. The S+5R+6C combination has the highest shear strength under normal stress of 80 kPa (62.9 kPa). The shear strength of soil with 2% cement and 5%, 10%, and 15% RHA, and soil with 4% cement addition with 10% and 15% RHA showed a lower shear strength than the control specimen (Figure 6C) because the less concentration of cement is unable to accelerate the flocculation process.

The cohesion and angle of internal friction of control and all soil-RHA-cement specimens are shown in Figure 6D. Compared to the control specimen, all mix types showed increased cohesive value. The S+5R+6C combination had the highest cohesive strength among all soil-RHA-cement mix types. On the contrary, the angle of internal friction of all soil-RHA-cement combination types decreased compared to untreated soil as the direct shear tests were performed after the initial setting of cement. The friction angle increased with cement content increment among the soil-RHA-cement mix types though the values were lower than the control specimen. However, it is expected that after the final set of cement and pozzolanic reactions of RHA, the angle of internal friction values may be higher than the control specimen. After mixing the RHA and cement with water in the soil, the flocculation process takes an instant to a few hours, the cement hydration occurs for one month, and pozzolanic reactions for months to a year (Sargent, 2015). Eliaslankaran *et al*. (2021) found that both cohesion and angle of internal friction significantly increased with curing days (7, 14, 28, 90 days) for soil-RHA-cement admixtures.

Conclusions

The investigation concluded that the shear strength of soil treated with RHA was affected by the initial cement setting under direct shear tests. The shear strength increased for the soil with 5-10% RHA and 4-6% cement content compared to the control specimen. The highest shear strength was observed for the S+5R+6C combination (62.9 kPa) under 80 kPa normal stress. The highest

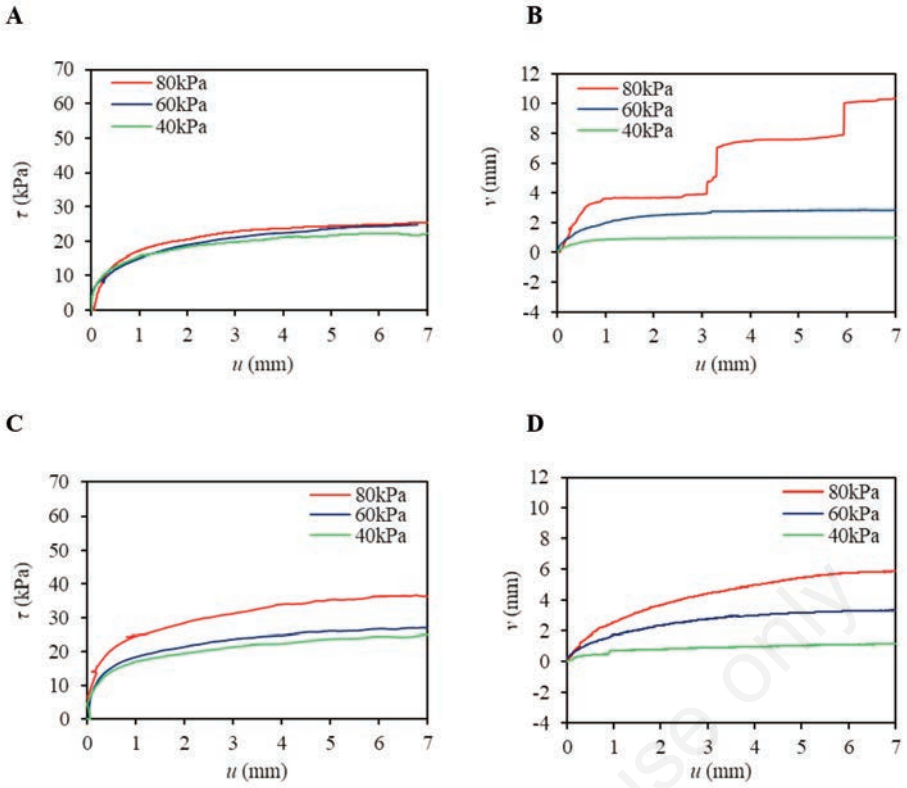

Figure 5. A) Shear stress (*τ*) *vs* shear displacement (*u*), and (B) vertical displacement (*v*) *vs* shear displacement (*u*) relationship of S+15R+2C specimen; C) shear stress (τ) *vs* shear displacement (*u*), and (D) vertical displacement (*v*) *vs* shear displacement (*u*) relationship of S+15R+4C specimen.

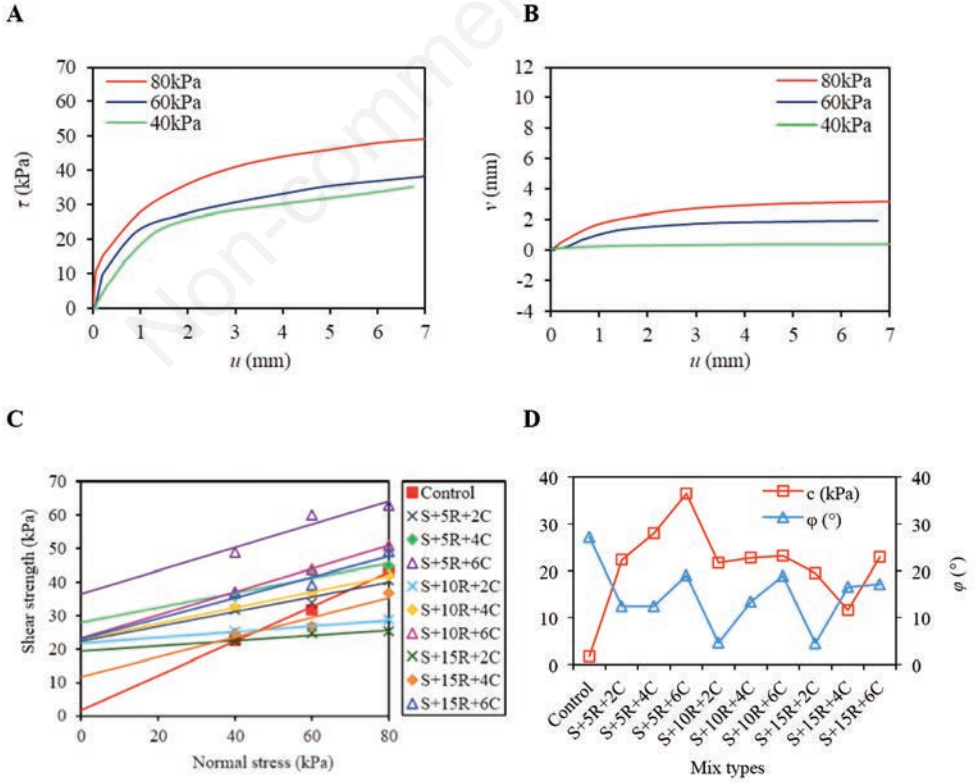

Figure 6. A) Shear stress (*τ*) *vs* shear displacement (*u*), and (B) vertical displacement (*v*) *vs* shear displacement (*u*) relationship of S+15R+6C specimen; C) variation of shear strength *vs* normal stress of control and various soil-RHA-cement combinations; D) variation of cohesion (*c*) and angle of internal friction (*φ*) of control and various soil-RHA-cement combinations.

vertical displacement was detected for the S+15R+2C specimen (10.3312 mm) under 80 kPa normal stress. Cohesion values of all soil-RHA-cement combinations were higher than in control specimens, but the angle of internal friction values of all combination types was lower than in untreated soil. The S+5R+6C combination can be used for the base and sub-base of rural roads and slope surface protection. As the shear strength varies with the variation of water content and curing time, future work is required considering varied water contents and curing periods.

References

Alhassan M., Alhaji M.M. 2017. Utilisation of rice husk ash for improvement of deficient soils in Nigeria: a review. Nigerian J. Technol. 36:386-94.

Ali F.H., Adnan A., Choy C.K. 1992. Geotechnical properties of a chemically stabilized soil from Malaysia with rice husk ash as an additive. Geotech. Geol. Eng. 10:117-34.

Basha E.A., Hashim R., Mahmud H.B., Muntohar A.S. 2005. Stabilization of residual soil with rice husk ash and cement. Constr. Build. Mater. 19:448-53.

Choobbasti A.J., Ghodrat H., Vahdatirad M.J., Firouzian S., Barari A., Torabi M., Bagherian A. 2010. Influence of using rice husk ash in soil stabilization method with lime. Front. Earth Sci. China. 4:471-80.

Dirgėlienė N., Skuodis Š., Grigusevičius A. 2017. Experimental and numerical analysis of direct shear test. Procedia Eng. 172:218-25.

Eliaslankaran Z., Daud N.N.N., Yusoff Z.M., Rostami V. 2021. Evaluation of the effects of cement and lime with rice husk ash as an additive on strength behavior of coastal soil. Mater. 14:1140.

Eslami A., Moshfeghi S., Molaabasi H., Eslami M.M. 2019. Piezocone and cone penetration test (CPTu and CPT) applications in foundation engineering. Butterworth-Heinemann.

Gunasekaran K., Annadurai R., Kumar P.S. 2013. Plastic shrinkage and deflection characteristics of coconut shell concrete slab. Constr. Build. Mater. 43:203-7.

Jamil M., Kaish A.B.M.A., Raman S.N., Zain M.F.M. 2013. Pozzolanic contribution of rice husk ash in cementitious system. Constr. Build. Mater. 47:588-93.

JGS 0561, 2010. Method for consolidated constant pressure direct box shear test on soils. pp 121-134 in Japanese Industrial Standard, Guidance and Basic - Soil Test, The Japanese Geotechnical Society. [in Japanese].

Jongpradist P., Homtragoon W., Sukkarak R., Kongkitkul W., Jamsawang P. 2018. Efficiency of rice husk ash as cementitious material in high-strength cement-admixed clay. Adv. Civ. Eng. 2018.

Kaur I. Jha J.N. 2016. Effects of rice husk ash - cement mixtures on stabilization of clayey soils, IJCA. Proceedings on International Conference on Advancements in Engineering and Technology, 8:30-33.

Khan M.M.H., Loh E.W.K., Singini P.T. 2016. Stabilization of tropical residual soil using rice husk ash and cement. Int. J. Appl. Environ. Sci. 11:73-87.

Khan R., Jabbar A., Ahmad I., Khan W., Khan A.N., Mirza J. 2012. Reduction in environmental problems using rice-husk ash in concrete. Constr. Build. Mater. 30:360-5.

Lee S.H., Hong K.N., Park J.K., Ko J. 2014. Influence of aggregate coated with modified sulfur on the properties of cement concrete. Mater. 7:4739-54.

Murthy V.N.S. 2002. Geotechnical engineering: principles and practices of soil mechanics and foundation engineering. CRC press, Boca Raton, FL, USA.

Nahar N., Hossain Z., Tamaki N. 2021. Optimum utilization of rice husk ash waste for ground improvement. Int. Agric. Eng. J. 30:1-10.

Nguyen D.T., Nguyen N.T. 2020. Effect of different types of rice husk ash on some geotechnical properties of cement-admixed soil. Iraqi Geol. J. 1-12.

Rachmawati S.H., Hossain Z., Shiau J. 2018. Agriculture land development using shell husk as recycle aggregate. Agric. Eng. Int. CIGR J. 20:45-51.

Rahman M.A. 1987. Effects of cement-rice husk ash mixtures on geotechnical properties of lateritic soils. Soils Found. 27:61-5.

Roy S., Bhalla S.K. 2017. Role of geotechnical properties of soil on civil engineering structures. Resour. Environ. 7:103-9.

Sargent P. 2015. The development of alkali-activated mixtures for soil stabilisation. In: Handbook of alkali-activated cements, mortars and concretes. Woodhead Publishing, Sawston, UK, pp. 555-604.

Thomas B.S. 2018. Green concrete partially comprised of rice husk ash as a supplementary cementitious material - A comprehensive review. Renew. Sustain. Energy Rev. 82:3913-23.